

1 Ancestral process for infectious disease outbreaks with superspreading

2 Xavier Didelot<sup>1,2,\*</sup>, David Helekal<sup>3</sup>, Ian Roberts<sup>2</sup>

3 <sup>1</sup> School of Life Sciences, University of Warwick, Coventry, United Kingdom

4 <sup>2</sup> Department of Statistics, University of Warwick, Coventry, United Kingdom

5 <sup>3</sup> Department of Immunology and Infectious Diseases, Harvard T. H. Chan School of Public Health,  
6 Boston, Massachusetts, USA

7 \* Corresponding author. Tel: 0044 (0)2476 572827. Email: `xavier.didelot@warwick.ac.uk`

8 Running title: Ancestry for outbreaks with superspreading

9 Keywords: infectious disease epidemiology modelling; offspring distribution; superspreading;  
10 outbreaks; Lambda-coalescent model; multiple mergers

## Abstract

When an infectious disease outbreak is of a relatively small size, describing the ancestry of a sample of infected individuals is difficult because most ancestral models assume large population sizes. Given a set of infected individuals, we show that it is possible to express exactly the probability that they have the same infector, either inclusively (so that other individuals may have the same infector too) or exclusively (so that they may not). To compute these probabilities requires knowledge of the offspring distribution, which determines how many infections each infected individual causes. We consider transmission both without and with superspreading, in the form of a Poisson and a Negative-Binomial offspring distribution, respectively. We show how our results can be incorporated into a new Lambda-coalescent model which allows multiple lineages to coalesce together. We call this new model the Omega-coalescent, we compare it with previously proposed alternatives, and advocate its use in future studies of infectious disease outbreaks.

# 1 Introduction

An outbreak of an infectious disease typically starts when a single or a small number of infected individuals appear within a susceptible population. Each infected individual may come in contact with and transmit the disease to each of the susceptible individuals, who will then become infected in their turn and spread the disease further. Most mathematical models of infectious diseases describe situations where the disease is at an equilibrium, when the number of infected individuals is high and/or with a significant part of the population already infected (Anderson and May 1991; Keeling and Rohani 2008). Here however we focus on the early stages of an epidemic, where the number of infected individuals is small and the number of susceptibles comparatively high and constant. In this situation it is useful to consider the number of new infections that each infected individual is likely to cause, and the probabilistic distribution for this number is often called the offspring distribution (Grassly and Fraser 2008). The mean of the offspring distribution is called the basic reproduction number  $R_0$  and has been given much attention especially since it determines how likely the outbreak is to spread, and how much effort would be needed to bring it under control (Fraser et al. 2004; Ferguson et al. 2006).

If we consider that all individuals are infectious for the same duration and with the same transmission rate, the offspring distribution is Poisson distributed with mean  $R_0$ , in which case the variance of the offspring distribution is also  $R_0$ . We would then say that there is no transmission heterogeneity. However, in practice there are many reasons why this may not be the case, with some individuals being infectious for longer than others, or being more infectious than others, or having more frequent contacts with susceptibles, or being less symptomatic and therefore less likely to reduce contact numbers, etc. All these factors cause the offspring distribution to be more dispersed than it would otherwise be, that is to have a variance greater than its mean  $R_0$ . A frequent choice to capture this overdispersion is to model the offspring distribution using a Negative-Binomial distribution with mean  $R_0$  and dispersion parameter  $r$  (Lloyd-Smith et al. 2005; Grassly and Fraser 2008). When  $r$  is close to zero the variance is high compared to the mean, whereas when  $r$  is high the variance becomes close to the mean. This transmission heterogeneity is often called superspreading, although this is perhaps misleading as it is the rule rather than the exception of how infectious diseases spread. Superspreading has indeed been described in many diseases (Woolhouse et al. 1997; Stein 2011; Kucharski and Althaus 2015; Wang et al. 2021), and most recently for SARS-CoV-2 (Wang et al. 2020; Lemieux et al. 2021; Gómez-Carballa et al. 2021; Du et al. 2022).

As an outbreak unfolds forward-in-time, a transmission tree is generated representing who-infected-

whom, in which each node is an infected individual and points towards a number of nodes distributed according to the offspring distribution. Here we consider the reverse problem of the transmission ancestry, going backward-in-time, from a sample of infected individuals, until reaching the last common transmission ancestor of the whole sample. Given a set of  $n$  sampled individuals, we show how to calculate the probability that a given subset of size  $k$  have the same infector, either inclusively (so that the remaining  $n - k$  may also have the same infector or not) or exclusively (so that none of the remaining  $n - k$  have the same infector). We start by considering the general case of an offspring distribution with arbitrary form, and then the specific cases of offspring distributions that follow a Poisson and a Negative-Binomial distribution. The main novelty of our approach is that we consider that the overall population size is small, but we show that in the limit where the population size is large, our results agree with several previous studies (Volz 2012; Koelle and Rasmussen 2012; Fraser and Li 2017). Finally, we show how our results can be incorporated into a new Lambda-coalescent model (Pitman 1999; Sagitov 1999; Donnelly and Kurtz 1999) and compare it with previously proposed models.

## 2 General offspring distribution case

Let time be measured in discrete units and denoted  $t$ . Each discrete value of  $t$  corresponds to a unique non-overlapping generation of infected individuals, so that individuals infected at  $t$  have offspring at  $t + 1$ , etc. Let  $N_t$  denote the number of infectious individuals at time  $t$ . Each of them creates a number  $s_{t,i}$  of secondary infections at time  $t + 1$ , following the offspring distribution  $\alpha_t(s)$ . The mean of this distribution is the basic reproduction number  $R_t$  and the variance is  $V_t$ . The total number of infected individuals at time  $t + 1$  is given by:

$$N_{t+1} = \sum_{i=1}^{N_t} s_{t,i} \quad (1)$$

### 2.1 Inclusive coalescence probability

We define the inclusive coalescence probability  $p_{k,t}(N_t, N_{t+1})$  as the probability that a specific set of  $k$  individuals from generation  $t + 1$  have the same infector in generation  $t$ , conditional on population sizes  $N_t$  and  $N_{t+1}$ . Given full information about offspring counts from individuals in generation  $t$ ,

80  $\mathbf{s}_t = (s_{t,1}, \dots, s_{t,N_t})$ , we have:

$$\begin{aligned}
 p_{k,t}(\mathbf{s}_t, N_t) &= \sum_{i=1}^{N_t} \frac{\binom{s_{t,i}}{k}}{\binom{N_{t+1}}{k}} \\
 &= \sum_{i=1}^{N_t} \frac{s_{t,i}!}{(s_{t,i} - k)!} \frac{(N_{t+1} - k)!}{N_{t+1}!}
 \end{aligned} \tag{2}$$

81 Full information  $\{s_{t,i}\}$  yields the population size  $N_{t+1}$  as shown in Equation 1, but this is not available  
 82 in practice. We can instead express the inclusive coalescence probability conditioning on the next  
 83 population size  $N_{t+1}$  by summing over possible offspring counts  $\mathbf{s}_t = (s_{t,1}, \dots, s_{t,N_t})$  conditional on the  
 84 total generation size. Let  $S_t^{-(1)} = (S_{t,2}, \dots, S_{t,N_t})$ :

$$\begin{aligned}
 p_{k,t}(N_t, N_{t+1}) &= \sum_{\mathbf{s}_t \in \mathbb{N}_0^{N_t}} \mathbb{P} \left[ \mathbf{S}_t = \mathbf{s}_t \middle| \sum_{i=1}^{N_t} S_{t,i} = N_{t+1} \right] p_{k,t}(\mathbf{s}_t, N_t) \\
 &= \sum_{\mathbf{s}_t \in \mathbb{N}_0^{N_t}} \mathbb{P} \left[ \mathbf{S}_t = \mathbf{s}_t \middle| \sum_{i=1}^{N_t} S_{t,i} = N_{t+1} \right] \sum_{i=1}^{N_t} \frac{\binom{s_{t,i}}{k}}{\binom{N_{t+1}}{k}} \\
 &= \sum_{i=1}^{N_t} \sum_{\mathbf{s}_t \in \mathbb{N}_0^{N_t}} \frac{\binom{s_{t,i}}{k}}{\binom{N_{t+1}}{k}} \mathbb{P} \left[ S_{t,1} = s_{t,1}, \mathbf{S}_t^{-(1)} = \mathbf{s}_t^{-(1)} \middle| \sum_{i=1}^{N_t} S_{t,i} = N_{t+1} \right] \\
 &= \frac{N_t}{\binom{N_{t+1}}{k}} \sum_{\mathbf{s}_t \in \mathbb{N}_0^{N_t}} \binom{s_{t,1}}{k} \mathbb{P} \left[ S_{t,1} = s_{t,1} \middle| \sum_{i=1}^{N_t} S_{t,i} = N_{t+1} \right] \\
 &\quad \times \mathbb{P} \left[ \mathbf{S}_t^{-(1)} = \mathbf{s}_t^{-(1)} \middle| S_{t,1} = s_{t,1}, \sum_{i=1}^{N_t} S_{t,i} = N_{t+1} \right] \\
 &= \frac{N_t}{\binom{N_{t+1}}{k}} \sum_{s_{t,1}=0}^{N_{t+1}} \binom{s_{t,1}}{k} \mathbb{P} \left[ S_{t,1} = s_{t,1} \middle| \sum_{i=1}^{N_t} S_{t,i} = N_{t+1} \right] \\
 &\quad \times \underbrace{\sum_{\mathbf{s}_t^{-(1)} \in \mathbb{N}_0^{N_t-1}} \mathbb{P} \left[ \mathbf{S}_t^{-(1)} = \mathbf{s}_t^{-(1)} \middle| \sum_{i=2}^{N_t} S_{t,i} = N_{t+1} - s_{t,1} \right]}_{=1} \\
 &= \frac{N_t}{\binom{N_{t+1}}{k}} \mathbb{E} \left[ \binom{S_{t,1}}{k} \middle| \sum_{i=1}^{N_t} S_{t,i} = N_{t+1} \right] \\
 &= N_t \frac{(N_{t+1} - k)!}{N_{t+1}!} \mathbb{E} \left[ \frac{S_{t,1}!}{(S_{t,1} - k)!} \middle| \sum_{i=1}^{N_t} S_{t,i} = N_{t+1} \right]
 \end{aligned} \tag{3}$$

85 The  $k$ -th falling factorial moments  $\mathbb{E}\left[\frac{S_{t,1}!}{(S_{t,1}-k)!} \mid \sum_{i=1}^{N_t} S_{t,i} = N_{t+1}\right]$  in Equation 3 can be readily obtained  
 86 by differentiating the probability generating function of  $S_{t,1} \mid (\sum_{i=1}^{N_t} S_{t,i} = N_{t+1})$ .

## 87 2.2 Exclusive coalescence probability

88 Generally, we observe a sample of individuals from each generation rather than the entire population.  
 89 In this case, we are interested in the exclusive coalescence probability  $p_{n,k,t}(N_t, N_{t+1})$  that a specific  
 90 subset of  $k$  individuals amongst  $n$  sampled individuals arose from a common infector one generation  
 91 in the past given knowledge of the total population sizes  $N_t$  and  $N_{t+1}$ . Let us first assume full  
 92 knowledge about offspring counts of the individuals at time  $t$  amongst the sample at time  $t+1$ ,  
 93 namely  $\mathbf{x}_t = (x_{t,1}, \dots, x_{t,N_t})$  such that  $x_{t,1} + \dots + x_{t,N_t} = n$ . Note that  $X_{t,i}$  does not follow the same  
 94 offspring distribution as  $S_{t,i}$ . We have:

$$\begin{aligned} p_{n,k,t}(\mathbf{X}_t = \mathbf{x}_t, N_t) &= \sum_{i=1}^{N_t} \frac{\binom{x_{t,i}}{k}}{\binom{n}{k}} \mathbb{I}\{x_{t,i} = k\} \\ &= \sum_{i=1}^{N_t} \frac{x_{t,i}!}{(x_{t,i}-k)!} \frac{(n-k)!}{n!} \mathbb{I}\{x_{t,i} = k\} \end{aligned} \quad (4)$$

95 Similarly to the inclusive coalescence probability in Equation 3, we can use this to evaluate the exclusive  
 96 probability given  $N_t$  and  $N_{t+1}$  by summing over possible parent offspring configurations (for  $k \leq n$ ):

$$\begin{aligned} p_{n,k,t}(N_t, N_{t+1}) &= \sum_{\mathbf{x}_t \in \mathbb{N}_0^{N_t}} \mathbb{P}\left[\mathbf{X}_t = \mathbf{x}_t \mid \sum_{i=1}^n X_{t,i} = n\right] p_{n,k,t}(\mathbf{x}_t, N_t) \\ &= \sum_{\mathbf{x}_t \in \mathbb{N}_0^{N_t}} \mathbb{P}\left[\mathbf{X}_t = \mathbf{x}_t \mid \sum_{i=1}^n X_{t,i} = n\right] \sum_{i=1}^{N_t} \frac{\binom{x_{t,i}}{k}}{\binom{n}{k}} \mathbb{I}\{x_{t,i} = k\} \\ &= \frac{N_t}{\binom{n}{k}} \sum_{\mathbf{x}_t \in \mathbb{N}_0^{N_t}} \binom{x_{t,1}}{k} \mathbb{P}\left[\mathbf{X}_t = \mathbf{x}_t \mid \sum_{i=1}^{N_t} X_{t,i} = n\right] \mathbb{I}\{x_{t,1} = k\} \\ &= \frac{N_t}{\binom{n}{k}} \sum_{\mathbf{x}_t^{-(1)} \in \mathbb{N}_0^{N_t-1}} \binom{k}{k} \mathbb{P}\left[X_{t,1} = k, \mathbf{X}_t^{-(1)} = \mathbf{x}_t^{-(1)} \mid \sum_{i=1}^{N_t} X_{t,i} = n\right] \\ &= \frac{N_t}{\binom{n}{k}} \mathbb{P}[X_{t,1} = k \mid \sum_{i=1}^{N_t} X_{t,i} = n] \underbrace{\sum_{\mathbf{x}_t^{-(1)} \in \mathbb{N}_0^{N_t-1}} \mathbb{P}\left[\mathbf{X}_t^{-(1)} = \mathbf{x}_t^{-(1)} \mid \sum_{i=1}^{N_t} X_{t,i} = n, X_{t,1} = k\right]}_{=1} \end{aligned}$$

$$= \frac{N_t}{\binom{n}{k}} \mathbb{P} \left[ X_{t,1} = k \middle| \sum_{i=1}^{N_t} X_{t,i} = n \right] \quad (5)$$

## 2.3 Complementarity of exclusive coalescence probabilities

If we consider one of the lines observed amongst a set of  $n$ , it can either remain uncoalesced with probability  $p_{n,1,t}(N_t, N_{t+1})$  or coalesce in an event of size  $k$  with probability  $p_{n,k,t}(N_t, N_{t+1})$  with any set of  $k - 1$  lines among the  $n - 1$  other lines, leading to the following complementarity equation:

$$\sum_{k=1}^n \binom{n-1}{k-1} p_{n,k,t}(N_t, N_{t+1}) = 1 \quad (6)$$

We can show that it is indeed satisfied by the formula in Equation 5:

$$\begin{aligned} \sum_{k=1}^n \binom{n-1}{k-1} p_{n,k,t}(N_t, N_{t+1}) &= \sum_{k=1}^n \binom{n-1}{k-1} \frac{N_t}{\binom{n}{k}} \mathbb{P} \left[ X_1 = k \middle| \sum_{i=1}^{N_t} X_i = n \right] \\ &= \sum_{k=1}^n N_t \frac{k}{n} \mathbb{P} \left[ X_1 = k \middle| \sum_{i=1}^{N_t} X_i = n \right] \\ &= \frac{N_t}{n} \sum_{k=0}^n k \mathbb{P} \left[ X_1 = k \middle| \sum_{i=1}^{N_t} X_i = n \right] \\ &= \frac{N_t}{n} \mathbb{E} \left[ X_1 \middle| \sum_{i=1}^{N_t} X_i = n \right] \\ &= \frac{1}{n} \sum_{i=1}^{N_t} \mathbb{E} \left[ X_i \middle| \sum_{i=1}^{N_t} X_i = n \right] \\ &= \frac{1}{n} \mathbb{E} \left[ \sum_{i=1}^{N_t} X_i \middle| \sum_{i=1}^{N_t} X_i = n \right] \\ &= 1 \end{aligned} \quad (7)$$

### 3 Poisson offspring distribution case

In this section we consider that the offspring distribution is  $\alpha_t = \text{Poisson}(R_t)$ . In this case, we have:

$$\sum_{i=1}^{N_t} S_{t,i} \sim \text{Poisson}(N_t R_t) \quad (8)$$

and the conditional distribution:

$$\begin{aligned} \mathbb{P}\left[S_{t,1} = s \mid \sum_{i=1}^{N_t} S_{t,i} = N_{t+1}\right] &= \frac{\mathbb{P}\left[S_{t,1} = s, \sum_{i=1}^{N_t} S_{t,i} = N_{t+1}\right]}{\mathbb{P}\left[\sum_{i=1}^{N_t} S_{t,i} = N_{t+1}\right]} \\ &= \frac{\alpha_t(s) \mathbb{P}\left[\sum_{i=2}^{N_t} S_{t,i} = N_{t+1} - s\right]}{\mathbb{P}\left[\sum_{i=1}^{N_t} S_{t,i} = N_{t+1}\right]} \\ &= \frac{\frac{R_t^s e^{-R_t}}{s!} \cdot \frac{((N_t - 1)R_t)^{N_{t+1} - s}}{(N_{t+1} - s)!}}{\frac{(N_t R_t)^{N_{t+1}} e^{-N_t R_t}}{N_{t+1}!}} \\ &= \binom{N_{t+1}}{s} \left(\frac{1}{N_t}\right)^s \left(1 - \frac{1}{N_t}\right)^{N_{t+1} - s} \end{aligned} \quad (9)$$

This is the probability mass function of a Binomial distribution and therefore we deduce that:

$$S_{t,1} \mid \left(\sum_{i=1}^{N_t} S_{t,i} = N_{t+1}\right) \sim \text{Binomial}\left(N_{t+1}, \frac{1}{N_t}\right) \quad (10)$$

The  $k$ -th falling factorial moments of  $X \sim \text{Binomial}(n, p)$  are (Potts 1953):

$$\mathbb{E}\left[\frac{X!}{(X - k)!}\right] = \binom{n}{k} p^k k! \quad (11)$$

By applying this formula to the Binomial distribution in Equation 10 and injecting into Equation 3, we deduce that the inclusive probability of coalescence for  $k$  lines is:



$$p_{k,t}(N_t, N_{t+1}) = \frac{1}{N_t^{k-1}} \quad (12)$$

109 In addition, following a similar reasoning as for Equation 10 we can show that:

$$X_{t,1} \left| \left( \sum_{i=1}^{N_t} X_{t,i} = n \right) \sim \text{Binomial} \left( n, \frac{1}{N_t} \right) \quad (13)$$

110 By injecting the probability mass function of this Binomial distribution into Equation 5 we deduce  
 111 that the exclusive probability of coalescence for  $k$  lines from a sample of  $n$  ( $n \geq k$ ) is:

$$p_{n,k,t}(N_t, N_{t+1}) = \frac{(N_t - 1)^{n-k}}{N_t^{n-1}} \quad (14)$$

112 It is interesting to note that neither the inclusive nor the exclusive coalescence probability depend on  
 113 the mean  $R_t$  of the Poisson offspring distribution or the size  $N_{t+1}$  of the population at time  $t+1$ . Both  
 114 only depend on the population size  $N_t$  at time  $t$ . The inclusive coalescent probability in Equation 12  
 115 can also be obtained conceptually by considering that among the  $k$  lines, the first one has an ancestor  
 116 with probability one, and the remaining  $k-1$  need to have the same ancestor among a set of  $N_t$  from  
 117 which they choose uniformly at random so that the probability of picking the same ancestor is  $1/N_t$ .  
 118 The exclusive coalescent probability in Equation 14 can be derived likewise by considering that in  
 119 addition to the above, each of the  $n-k$  other lines need to choose a different ancestor, which happens  
 120 with probability  $(N_t - 1)/N_t$ . Figure 1 illustrates the inclusive and exclusive coalescence probabilities  
 121 for a set of size  $k = 1$  to  $k = 10$  amongst a total of  $n = 10$  observed individuals, in a population of size  
 122  $N_t = 10$ ,  $N_t = 20$  or  $N_t = 30$ .

## 123 4 Negative-Binomial offspring distribution case

124 In this section we consider that the offspring distribution is Negative-Binomial, a distribution often  
 125 used to model superspreading individuals (Lloyd-Smith et al. 2005) and which can also be used to model  
 126 superspreading events (Craddock et al. 2025). Let  $\alpha_t = \text{Negative-Binomial}(r, p)$  with parameters  $(r, p)$   
 127 set by moment-matching the mean  $R_t$  and variance  $V_t$  of the offspring distribution which are assumed  
 128 constant over time. The resulting parameters for this distribution are  $r = R_t^2/(V_t - R_t)$  and  $p = R_t/V_t$ .

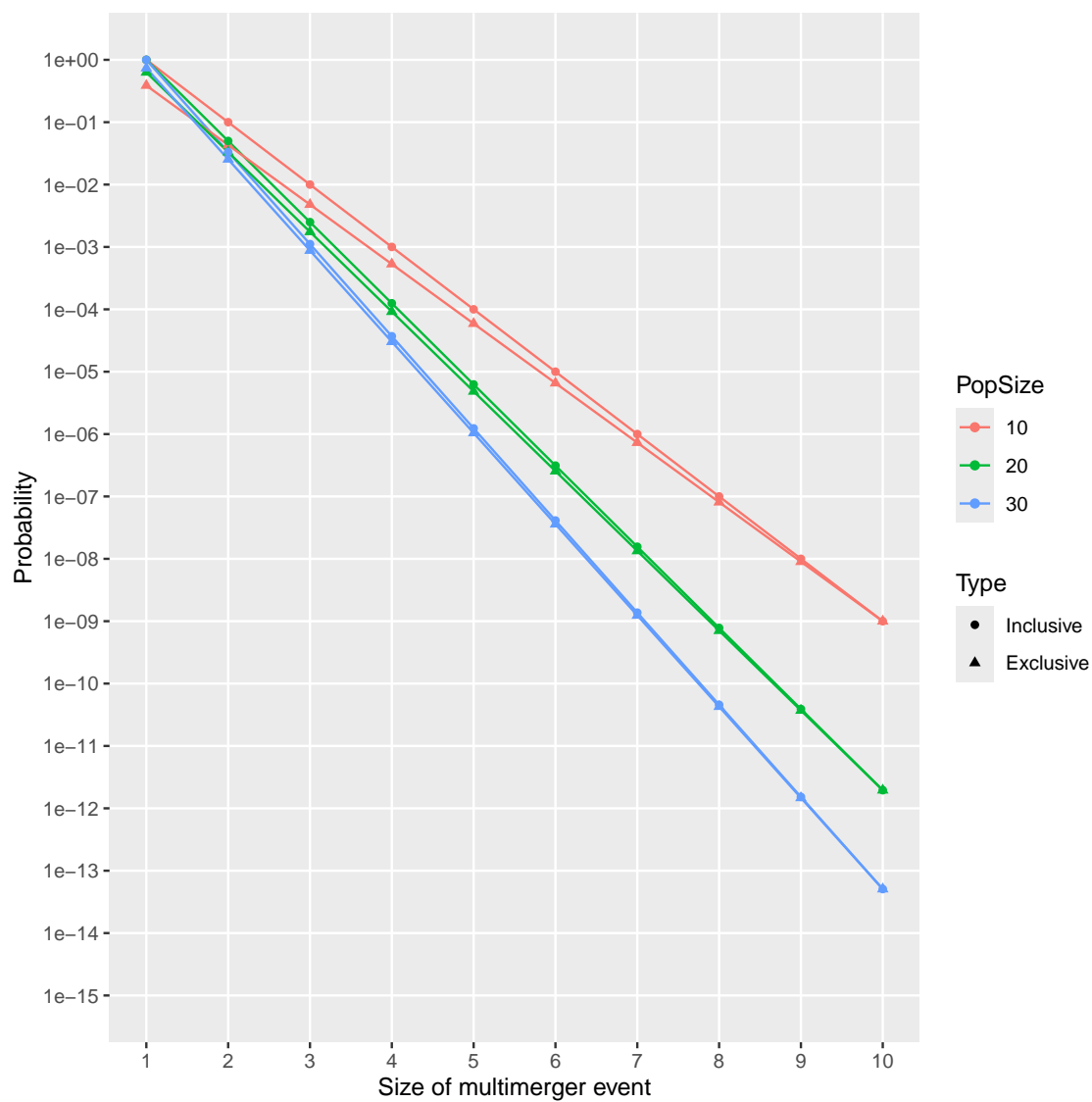


Figure 1: Inclusive and exclusive coalescence probabilities for the Poisson case.

129 In this case, we have:

$$\sum_{i=1}^{N_t} S_{t,i} \sim \text{Negative-Binomial}(N_t r, p) \quad (15)$$

130 and similarly to the Poisson offspring distribution case we identify that the conditional distribution of

131  $S_{t,1} | \sum_{i=1}^{N_t} S_{t,i}$  is as follows:

$$\begin{aligned} \mathbb{P}\left[S_{t,1} = s \mid \sum_{i=1}^{N_t} S_{t,i} = N_{t+1}\right] &= \frac{\alpha_t(s) \cdot \mathbb{P}\left[\sum_{i=2}^{N_t} S_{t,i} = N_{t+1} - s\right]}{\mathbb{P}\left[\sum_{i=1}^{N_t} S_{t,i} = N_{t+1}\right]} \\ &= \frac{\frac{\Gamma(r+s)}{s! \Gamma(r)} (1-p)^s p^r \cdot \frac{\Gamma((N_t-1)r + (N_{t+1}-s))}{(N_{t+1}-s)! \Gamma((N_t-1)r)} (1-p)^{N_{t+1}-s} p^{(N_t-1)r}}{\frac{\Gamma(N_t r + N_{t+1})}{N_{t+1}! \Gamma(N_t r)} (1-p)^{N_{t+1}} p^{N_t r}} \\ &= \frac{N_{t+1}!}{s! (N_{t+1}-s)!} \frac{\Gamma(r+s) \Gamma((N_t-1)r + (N_{t+1}-s))}{\Gamma(N_t r + N_{t+1})} \frac{\Gamma(N_t r)}{\Gamma(r) \Gamma((N_t-1)r)} \\ &= \binom{N_{t+1}}{s} \frac{B(s+r, N_{t+1}-s + (N_t-1)r)}{B(r, (N_t-1)r)} \end{aligned} \quad (16)$$

132 where  $B(x, y)$  denotes the Beta function defined as  $B(x, y) = \Gamma(x)\Gamma(y)/\Gamma(x+y)$ . This is the probability  
133 mass function of a Beta-Binomial distribution and therefore we deduce that:

$$S_{t,1} \mid \left( \sum_{i=1}^{N_t} S_{t,i} = N_{t+1} \right) \sim \text{Beta-Binomial}(N_{t+1}, r, (N_t-1)r) \quad (17)$$

134 The  $k$ -th falling factorial moments of  $X \sim \text{Beta-Binomial}(n, \alpha, \beta)$  are (Tripathi et al. 1994):

$$\mathbb{E}\left[\frac{X!}{(X-k)!}\right] = \binom{n}{k} \frac{B(\alpha+k, \beta)k!}{B(\alpha, \beta)} \quad (18)$$

135 By applying this formula to the Beta-Binomial distribution in Equation 17 and injecting into Equation  
136 3, we deduce that the inclusive probability of coalescence for  $k$  lines is:

$$p_{k,t}(N_t, N_{t+1}) = \frac{B(N_t r + 1, r + k)}{B(r + 1, N_t r + k)} \quad (19)$$

137 In addition, following a similar reasoning as for Equation 17, we can show that:

$$X_{t,1} \left| \left( \sum_{i=1}^{N_t} X_{t,i} = n \right) \right. \sim \text{Beta-Binomial}(n, r, (N_t - 1)r) \quad (20)$$

138 By injecting the probability mass function of this Beta-Binomial distribution into Equation 5 we deduce  
 139 that the exclusive probability of coalescence for  $k$  lines is:

$$p_{n,k,t}(N_t, N_{t+1}) = \frac{N_t B(k + r, n - k + N_t r - r)}{B(r, N_t r - r)} \quad (21)$$

140 It is interesting to note that as for the Poisson case, the inclusive and exclusive coalescence probabilities  
 141 do not depend on the size  $N_{t+1}$  of the population at time  $t + 1$ . They both depend on the Negative-  
 142 Binomial offspring distribution only through the dispersion parameter  $r$ . If we consider that  $r$  is large  
 143 in Equations 19 and 21, we can derive that the asymptotic behaviour is the same as in the Poisson  
 144 case shown in Equations 12 and 14. For example this can be derived by rewriting the Beta functions  
 145 using Gamma functions, and using the following form of Stirling's approximation:

$$\lim_{a \rightarrow \infty} \frac{\Gamma(a + b)}{\Gamma(a)} = a^b e^{-b} \quad (22)$$

146 Figure 2 illustrates the inclusive and exclusive coalescence probabilities for the Negative-Binomial case  
 147 for a set of size  $k = 1$  to  $k = 10$  amongst a total of  $n = 10$  observed lines, in a population with  
 148 size  $N_t = 20$ . Several Negative-Binomial offspring distributions are compared, all of which have the  
 149 same mean  $R_t = 2$ , and with the dispersion parameter equal to  $r = 0.1$ ,  $r = 1$ ,  $r = 10$  and  $r = 100$   
 150 (Figure 2A). When  $r = 1$  the Negative-Binomial reduces to a Geometric distribution. When  $r$  is high  
 151 the dispersion is low and the Negative-Binomial case behaves almost like the Poisson case for both  
 152 the inclusive (Figure 2B) and the exclusive coalescence probabilities (Figure 2C). When  $r$  is lower the  
 153 dispersion of the offspring distribution increases, so that both the inclusive and exclusive probabilities  
 154 of larger multiple merger events are increased compared to the Poisson case. In particular, when  
 155  $r = 0.1$  we see that the exclusive probability can increase with the size of the event considered (Figure  
 156 2C). This happens because the probability is not much lower for the common ancestor having say 10  
 157 rather than 9 offspring, while on the other hand if the event is of size 9 only then another individual  
 158 in the generation of the ancestor needs to have had at least one sampled offspring.

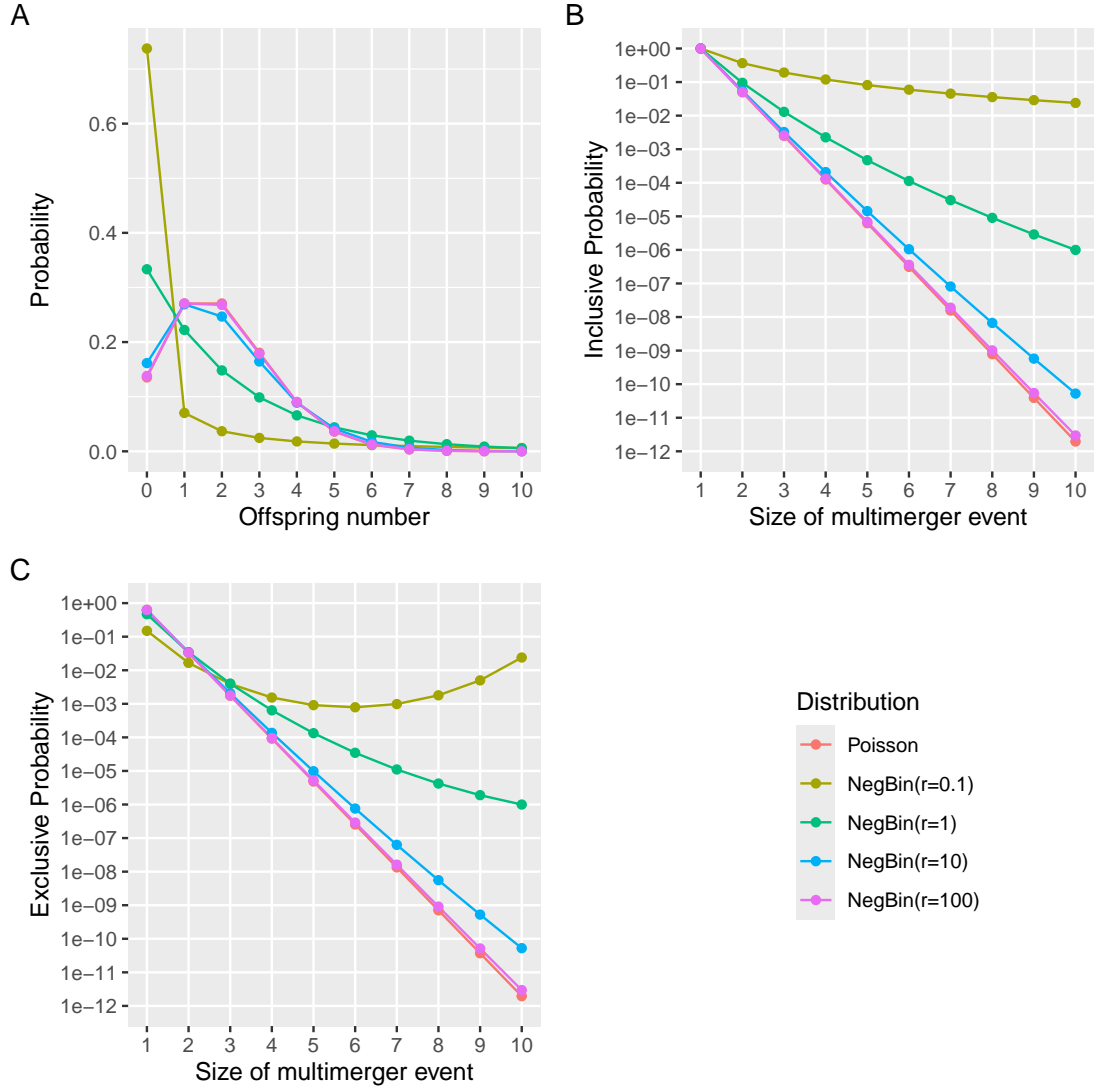


Figure 2: (A) Offspring distributions with mean  $R_t = 2$ . (B) Inclusive probability of coalescence for  $N_t = 20$  and  $n = 10$ . (C) Exclusive probability of coalescence for  $N_t = 20$  and  $n = 10$ .

## 5 Limit when the population size is large

Here we consider that the population size  $N_t$  is fixed and large, so that we can show the connections between our results and several previous studies on the ancestral process of infectious diseases. In the Poisson case, from Equations 12 and 14 we can see that both inclusive and exclusive probabilities are of order  $\mathcal{O}(N_t^{1-k})$ . We can therefore ignore events with  $k > 2$  and retain only the events with  $k = 2$ , which means that there are only binary coalescent events and no multiple merger events. The binary coalescent events occur with the same inclusive and exclusive probabilities:

$$p_{2,t}(N_t, N_{t+1}) = p_{n,2,t}(N_t, N_{t+1}) = \frac{1}{N_t} \quad (23)$$

For the Negative-Binomial case, from Equations 19 and 21 we can rewrite using Gamma functions and apply the form of Stirling's equation given in Equation 22 to show that once again both inclusive and exclusive probabilities are also of order  $\mathcal{O}(N_t^{1-k})$ . We can therefore once again ignore events with  $k > 2$  and retain only the events with  $k = 2$  which occur with the same inclusive and exclusive probabilities:

$$p_{2,t}(N_t, N_{t+1}) = p_{n,2,t}(N_t, N_{t+1}) = \frac{r+1}{N_t r + 1} \approx \frac{r+1}{N_t r} \quad (24)$$

Koelle and Rasmussen (2012) derived the rates of coalescence of two lineages for several epidemiological models, assuming a large population at equilibrium. For each model they use the equation  $N_e = N/\sigma^2$  to relate the effective population size  $N_e$  to the actual population size  $N$  and the variance  $\sigma^2$  in the number of offspring. This relationship was first established by Kingman (1982a) to derive the backward-in-time coalescent model from the forward-in-time Cannings exchangeable models (Cannings 1974). This result implies that the rate of coalescence for two lineages is  $1/N_e = \sigma^2/N$ . From Equation 24 we can take  $R_t = 1$  to achieve equilibrium of the population size and the method of moments estimator  $r = R_t^2/(V_t - R_t) = 1/(V_t - 1)$  to deduce the equivalent result  $p_{2,t}(N_t, N_{t+1}) = V_t/N_t$ .

Volz (2012) showed that the rate of coalescence for two lineages under a continuous-time epidemic coalescent model is  $2f(t)/I(t)^2$  where  $f(t)$  is the incidence of the disease and  $I(t)$  its prevalence. Setting in this formula the prevalence as  $I(t) = N_{t+1} = N_t R_t$  and the incidence as  $f(t) = R_t I(t) = R_t^2 N_t$  we get a coalescent rate of  $2/N_t$ . To apply our methodology we need to consider that the offspring distribution is Geometric, since the epidemiological models considered have successes (transmission) happening until the first failure (removal). We therefore set  $r = 1$  in Equation 24 to make the Negative-

184 Binomial offspring distribution reduce to a Geometric distribution and the same result follows.

185 Fraser and Li (2017) calculated the effective population size  $N_e(t)$  as a function of the actual population  
186 size  $N(t)$  and the mean and variance of the offspring distribution  $R$  and  $\sigma^2$ . This formula was used to  
187 estimate the dispersion parameter of a Negative-Binomial offspring distribution from genetic data (Li  
188 et al. 2017). Using our notations, their formula is equivalent to the inclusive coalescence probability  
189 for two lineages:

$$p_{2,t}(N_t, N_{t+1}) = \frac{V_t/R_t + R_t - 1}{N_t R_t} \quad (25)$$

190 In the Poisson case we have  $V_t = R_t$  so that Equation 25 simplifies to  $1/N_t$  which agrees with Equation  
191 23. In the Negative-Binomial case we have  $V_t/R_t = 1/p = 1 + R_t/r$  so that Equation 25 simplifies to  
192  $(r+1)/(N_t r)$  which agrees with our Equation 24. Conversely, if we substitute the method of moments  
193 estimator  $r = R_t^2/(V_t - R_t)$  in Equation 24 we obtain the Equation 25 originally from Fraser and Li  
194 (2017).

## 195 6 Definition of a new Lambda-coalescent model

196 The coalescent model (Kingman 1982a,b) describes the ancestry of a sample from a large population  
197 evolving according to many forward-in-time models such as the Wright-Fisher model (Wright 1931;  
198 Fisher 1930), the Moran model (Moran 1958) and the Cannings exchangeable model (Cannings 1974).  
199 Since the coalescent considers a large population in which each individual only has a number of offspring  
200 that is small compared to the population size, coalescent trees are always binary and do not feature  
201 multiple mergers, making them unsuitable to represent the ancestry of outbreaks considered in this  
202 study. However, if the population size is small in any of the aforementioned forward-in-time models,  
203 multiple mergers can occur, where more than two sampled individuals have the same ancestor. The  
204 Lambda-coalescent model is an extension of the coalescent model that allows for such multiple merger  
205 events (Pitman 1999; Sagitov 1999; Donnelly and Kurtz 1999).

206 A Lambda-coalescent model is defined by a probability measure  $\Lambda(dx)$  on the interval  $[0, 1]$ , from which  
207 we deduce the rate  $\lambda_{n,k}$  at which any subset of  $k$  lineages within a set of  $n$  observed lineages coalesce:

$$\lambda_{n,k} = \int_0^1 x^{k-2} (1-x)^{n-k} \Lambda(dx) \quad (26)$$

208 The Beta-coalescent (Schweinsberg 2003) is a specific type of Lambda-coalescent that has been used  
 209 recently in several studies analysing genetic data from infectious disease agents (Hoscheit and Pybus  
 210 2019; Menardo et al. 2021; Helekal et al. 2025; Zhang and Palacios 2024). The Beta-coalescent model  
 211 has a single parameter  $\alpha \in [0, 2]$  and is defined as:

$$\Lambda(dx) = \frac{x^{1-\alpha} (1-x)^{\alpha-1}}{B(2-\alpha, \alpha)} dx \quad (27)$$

212 By combining Equations 26 and 27 we deduce that:

$$\lambda_{n,k} = \frac{B(k-\alpha, n-k+\alpha)}{B(2-\alpha, \alpha)} \quad (28)$$

213 Special cases of the Beta-coalescent include  $\alpha = 2$  corresponding to the Kingman coalescent,  $\alpha = 1$   
 214 which is known as the Bolthausen-Sznitman coalescent and  $\alpha = 0$  for which the phylogeny is always  
 215 star-shaped.

216 We now define a new Lambda-coalescent based on the Negative-Binomial case described previously.  
 217 We call this new Lambda-coalescent model the Omega-coalescent (where Omega stands for outbreak).  
 218 For ease of comparison with other coalescent models, we consider that time is continuous and  
 219 that the population size remains constant equal to  $N_t = N$ . The exclusive coalescent probability  
 220  $p_{n,k,t}(N_t, N_{t+1})$  in the Negative-Binomial case given by Equation 21 can be used to determine the  
 221 corresponding rate of the Omega-coalescent, if we consider that the probability of each event in discrete  
 222 time is equal to the constant rate of this event happening in continuous time:

$$\lambda_{n,k} = p_{n,k,t}(N_t = N, N_{t+1} = N) = \frac{NB(k+r, n-k+Nr-r)}{B(r, Nr-r)} \quad (29)$$

223 Note that this equation implies that continuous time is measured approximately in number of  
 224 transmission generations. For example to measure time in decimal days instead, the time scale would  
 225 need to be multiplied by the mean of the generation time distribution measured in days (Svensson  
 226 2007). From Equations 26 and 29 we can deduce the probability measure associated with the Omega-



227 coalescent:

$$\Lambda(dx) = \frac{Nx^{r+1}(1-x)^{Nr-r-1}}{B(r, Nr-r)}dx \quad (30)$$

228 For a Lambda-coalescent model to be consistent, when a multiple merger of size  $k$  amongst  $n$  lineages  
 229 occurs, if an additional lineage is revealed it must either take part in the multiple merger or remain  
 230 unaffected (Berestycki 2009). This implies that the rates must satisfy:

$$\lambda_{n,k} = \lambda_{n+1,k} + \lambda_{n+1,k+1} \quad (31)$$

231 This consistency property is easily verified for the Beta-coalescent in Equation 28 and likewise for the  
 232 Omega-coalescent in Equation 29, in both cases using recursive properties of the Beta functions used  
 233 in the respective definitions.

234 The Omega-coalescent has two parameters: the constant population size  $N$  and the dispersion  
 235 parameter  $r$ . In order to compare the Omega-coalescent defined in Equation 29 with other models  
 236 such as the Beta-coalescent defined in Equation 28, we consider the distribution of the size  $k$  of the  
 237 next event among a set of  $n$  lineages. For any Lambda-coalescent this can be computed as:

$$p(k|n) = \frac{\binom{n}{k}\lambda_{n,k}}{\sum_{i=2}^n \binom{n}{i}\lambda_{n,i}} \quad (32)$$

238 Figure 3 compares this distribution for  $n = 10$  in the Beta-coalescent with parameter  $\alpha \in \{0.5, 1, 1.5\}$   
 239 and for the Omega-coalescent with parameters  $N \in \{10, 20, 30\}$  and  $r \in \{0.1, 1, 10\}$ . In the Beta-  
 240 coalescent, the distribution shifts towards more larger multiple merger events as the parameter  $\alpha$   
 241 decreases. In the Omega-coalescent a wider range of behaviours is obtained when varying the two  
 242 parameters  $N$  and  $r$ . For a given value of  $N$ , decreasing the value of  $r$  results in more larger events.  
 243 Conversely, for a given value of  $r$  we can see that increasing the value of  $N$  reduces the probability of  
 244 larger events.

245 Genealogies can be simulated from the Omega-coalescent model defined in Equation 29 using the same  
 246 algorithm as for other Lambda-coalescent models (Pitman 1999). Given  $n$  lineages, the next coalescent  
 247 event happens after a time that is exponentially distributed with rate  $\sum_{i=2}^n \binom{n}{i}\lambda_{n,i}$ , the size  $k$  of this  
 248 event is drawn according to Equation 32, and the  $k$  lineages that coalesce are chosen uniformly amongst  
 249 the  $n$  lineages. This process is repeated iteratively until all lineages have coalesced. Figure 4 shows  
 250 examples of trees simulated for a sample of size  $n = 20$ , constant population size  $N = 30$  and dispersion

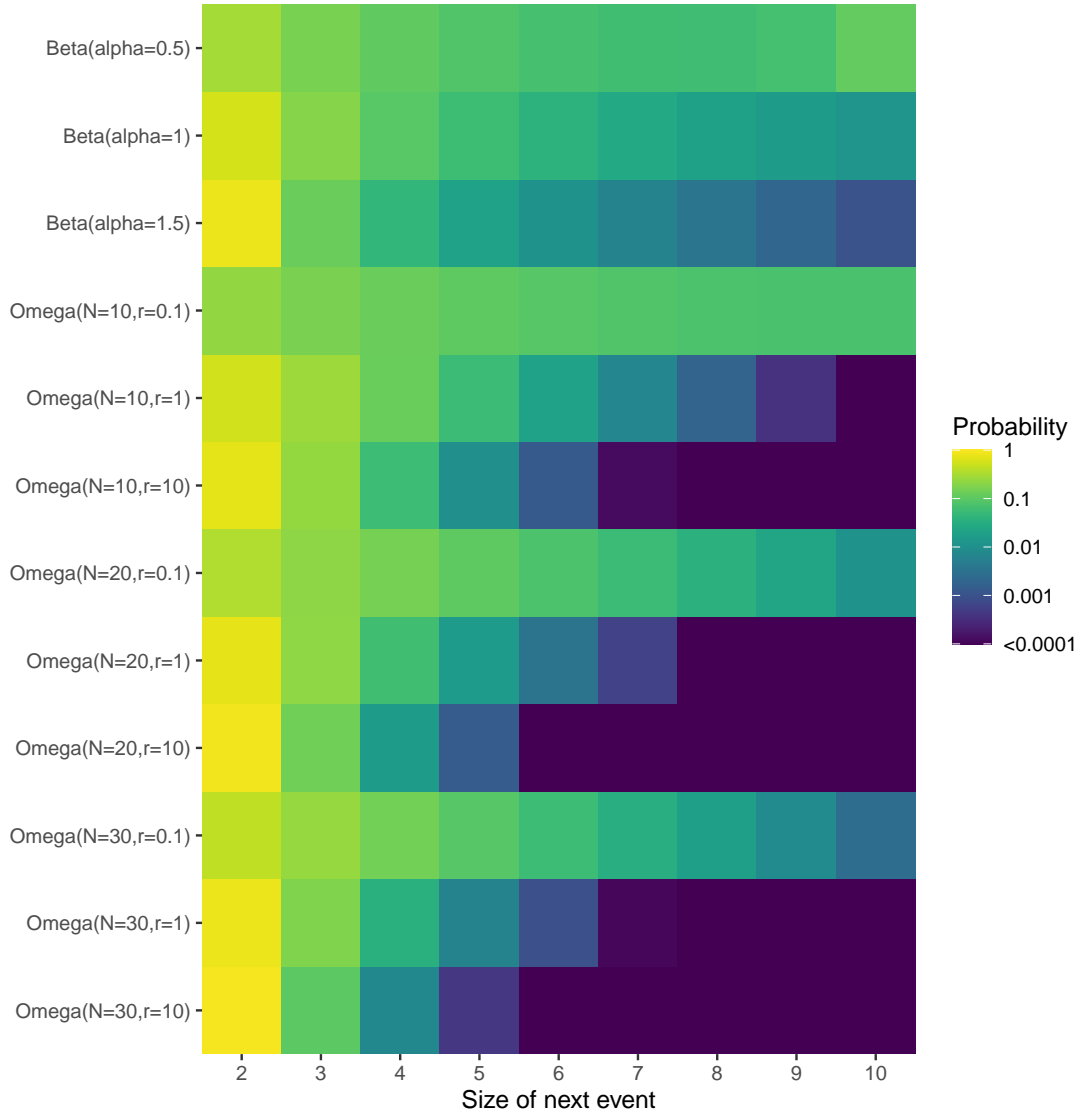


Figure 3: Distribution of the size of the next event among a set of  $n = 10$  lineages, compared between the Beta-coalescent and the Omega-coalescent model with various parameters.

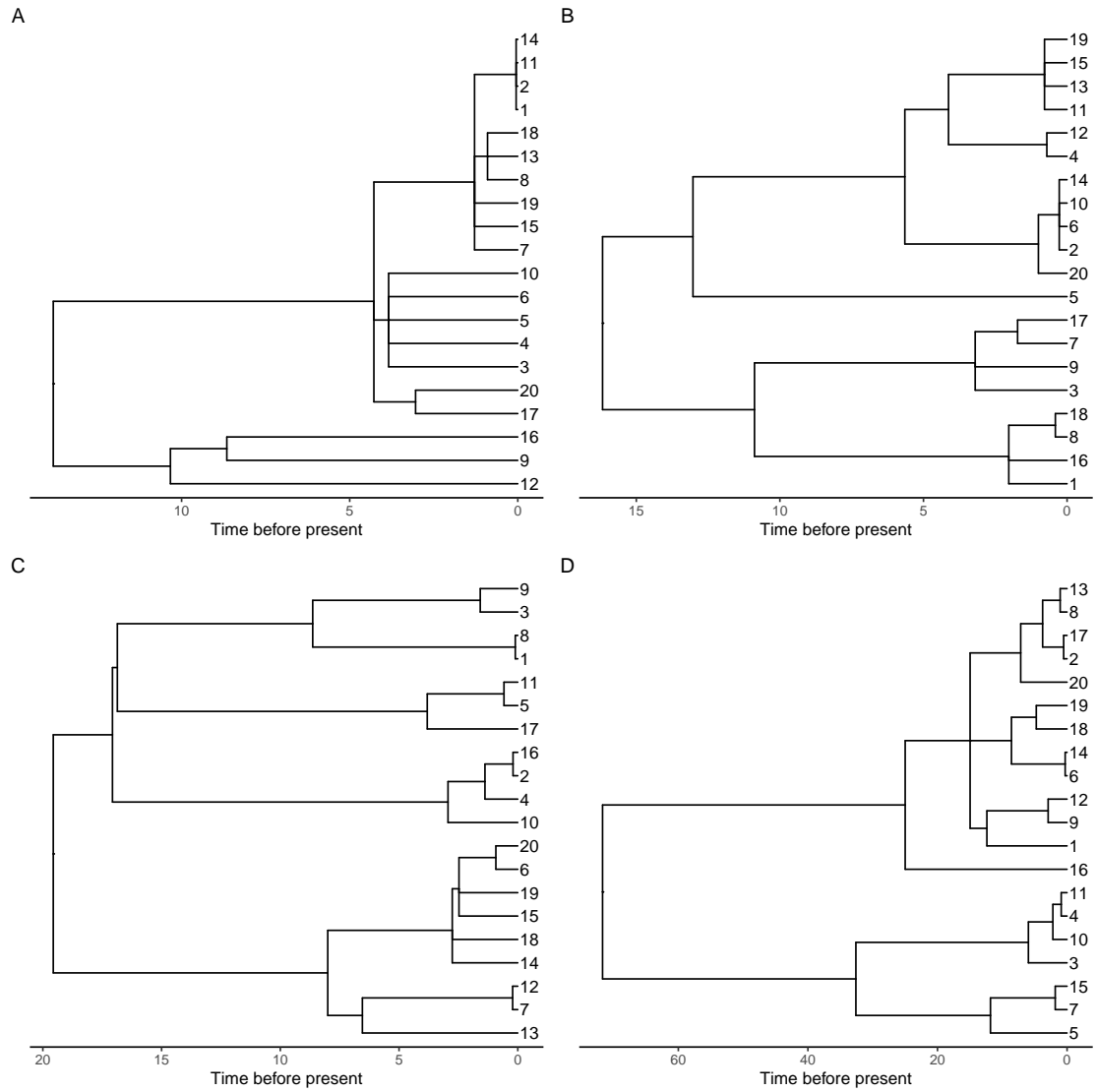


Figure 4: Example of trees simulated under the Omega-coalescent with  $r = 0.1$  (A),  $r = 1$  (B),  $r = 10$  (C) and  $r = 100$  (D).

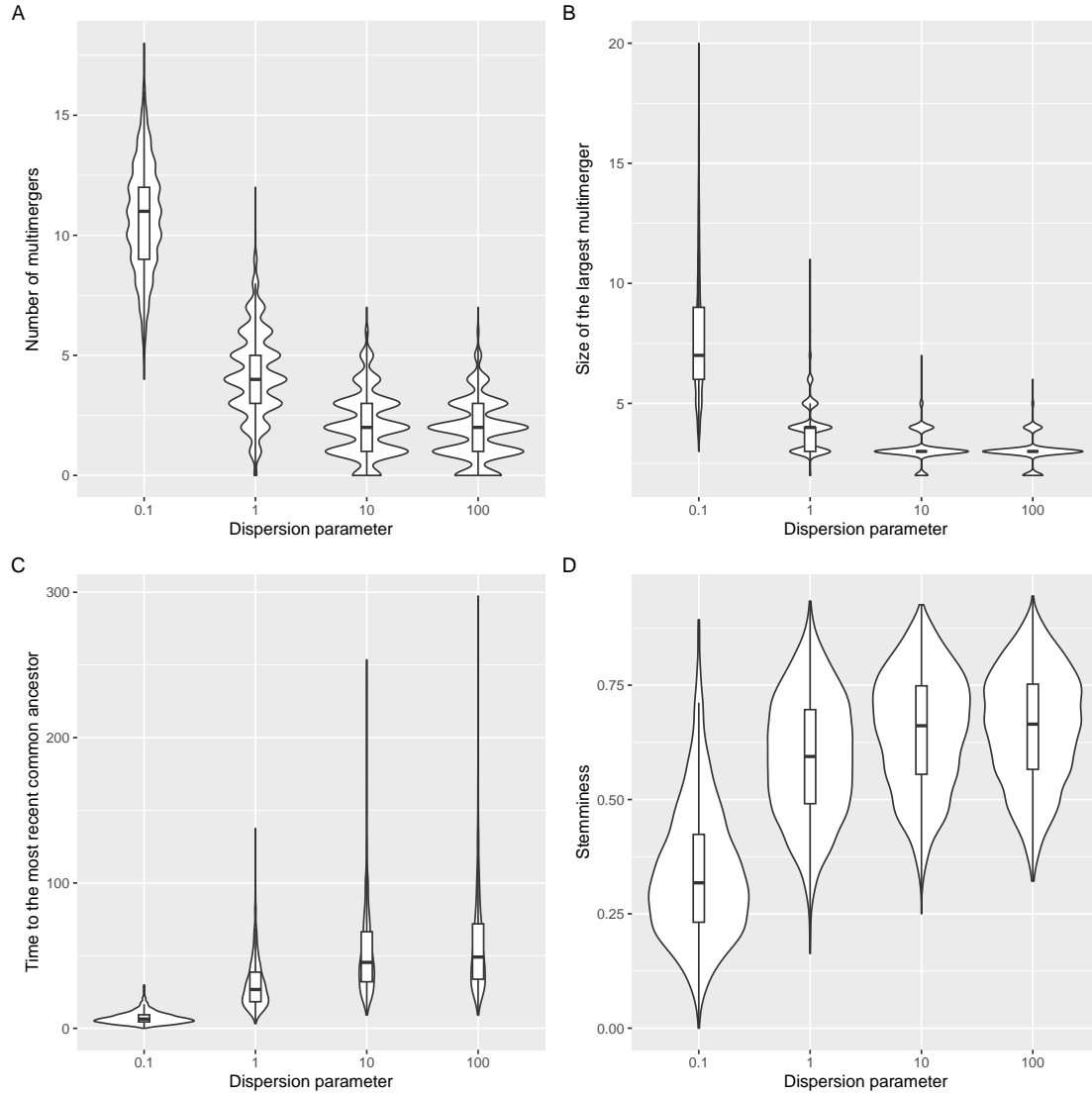


Figure 5: Summary statistics for trees simulated under the Omega-coalescent with  $r = 0.1$ ,  $r = 1$ ,  $r = 10$  and  $r = 100$ , namely number of multiple mergers (A) the size of the largest multiple merger (B), the time to the most recent common ancestor (C) and the stemminess (D).

parameter  $r \in \{0.1, 1, 10, 100\}$ . It is already clear from these single realisations that the lower values of  $r$  result in trees with more larger multiple merger events and lower time to the most recent common ancestor, but to quantify these properties we need to consider many trees. Figure 5 shows summary statistics for 10,000 trees simulated in the same conditions as the individual trees shown in Figure 4. As the dispersion parameter increases from  $r = 0.1$  to  $r = 100$  multiple merger events become less and less likely and less large (Figure 5A and B), and the time to the most recent common ancestor increases (Figure 5C). Furthermore, the stemminess of the tree increases, which is defined as the sum of lengths of internal branches divided by the total sum of branch lengths (Figure 5D). Stemminess is usually taken as a sign of population size dynamics (Fiala and Sokal 1985; Didelot et al. 2009), which would be misleading here since all simulations assumed a constant population size.

## 7 Parameter inference

Let us now consider a genealogy  $T$  with  $n$  leaves and  $c$  coalescent nodes, with  $t_0 = 0$  the sampling time,  $t_1, \dots, t_c$  the times of the coalescent nodes in increasing order and  $k_i$  the number of lineages coalescing at time  $t_i$ . The number of lineages existing between time  $t_{i-1}$  and  $t_i$  is then  $n_i = n - \sum_{j=1}^{i-1} k_j$ . Under a Lambda-coalescent model, the genealogy  $T$  has likelihood:

$$p(T|\Lambda) = \prod_{i=1}^c \lambda_{n_i, k_i} \exp \left( - \sum_{j=2}^{n_i} \binom{n_i}{j} \lambda_{n_i, j} (t_i - t_{i-1}) \right) \quad (33)$$

Note that in Equation 33 the term  $\binom{n_i}{k_i}$  term from the coalescent rate cancels out with its reciprocal from the probability of sampling  $k_i$  specific lineages to coalesce within a set of  $n_i$ . Estimating the lambda measure from Equation 26 in general is a difficult problem (Koskela 2018; Miró Pina et al. 2023). Here however we focus on estimation under the Omega-coalescent model, where the  $\lambda_{n,k}$  terms are given by Equation 29. There are therefore two parameters to estimate which have direct and important biological meaning: the effective population size  $N$  (which remains constant) and the dispersion parameter  $r$  of the Negative-Binomial offspring distribution. We perform estimation simply by maximising the likelihood in Equation 33, using the Brent algorithm (Brent 1971) when estimating a single parameter and the L-BFGS-B algorithm (Byrd et al. 1995) when estimating both parameters.

We simulated 100 genealogies from the Omega-coalescent model each of which had  $n = 100$  leaves, with parameter  $N$  drawn uniformly at random between 100 and 500 and parameter  $r$  drawn uniformly

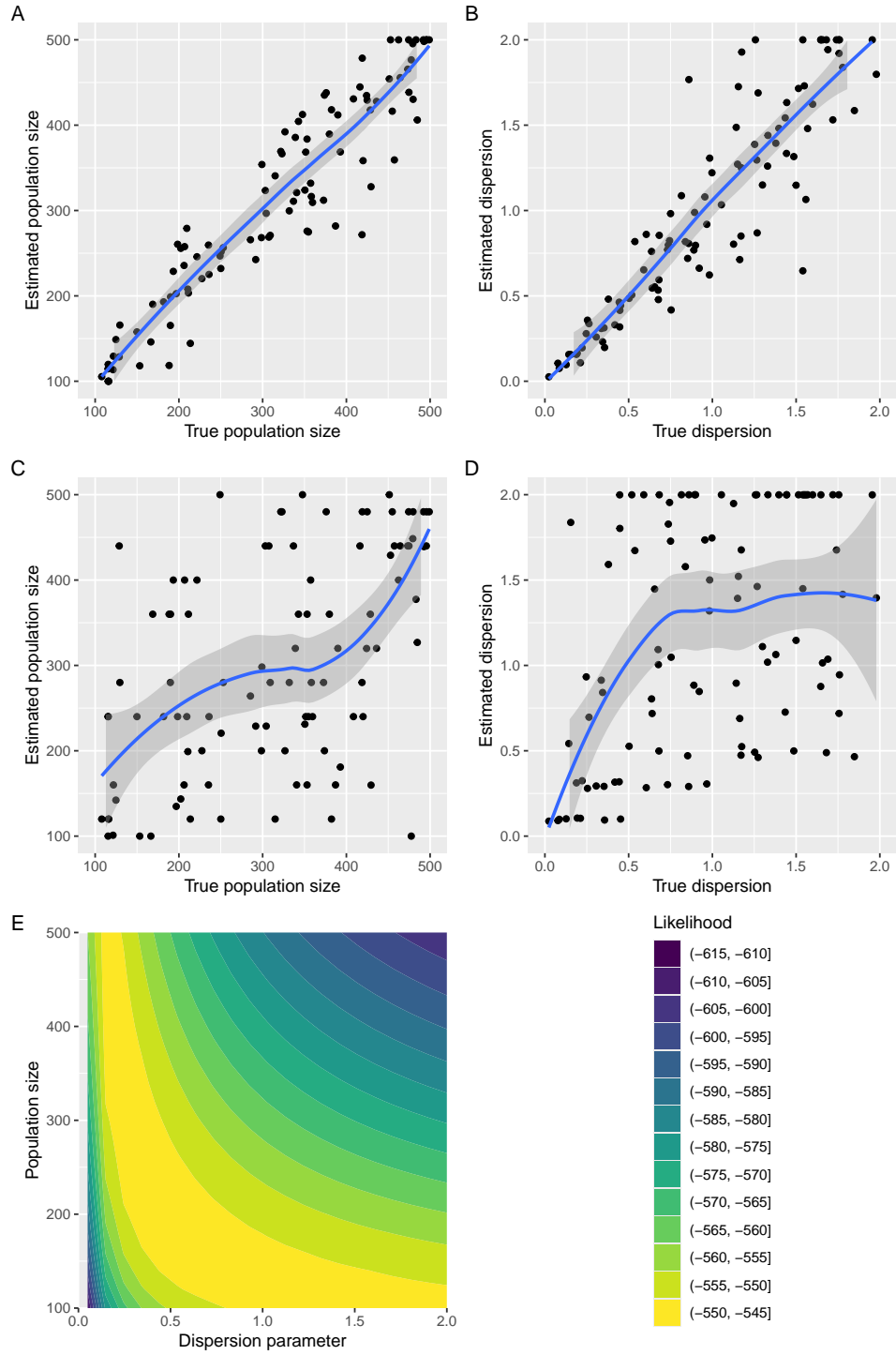


Figure 6: Maximum likelihood estimation of parameters. (A) Estimation of the population size given the dispersion parameter. (B) Estimation of the dispersion parameter given the population size. (C and D) Joint estimation of both the population size and dispersion parameters. (E) Example of likelihood surface as a function of both parameters.

277 at random between 0.01 and 2. If we assume knowledge of the dispersion parameter, then estimating  
 278 the population size works really well (Figure 6A). Conversely we obtain good result when estimating  
 279 the dispersion parameter given a known population size (Figure 6B). However, attempting to estimate  
 280 both parameters at the same time performed significantly less well (Figures 6C and D). To illustrate  
 281 the cause of this, we consider a simulation for which the true parameters were  $N = 200$  and  $r = 0.5$ ,  
 282 and we construct the likelihood surface (Figure 6E). This shows a strong inverse tradeoff between the  
 283 two parameters, which is why it is harder to infer both parameters jointly. This poor identifiability  
 284 is analogous to the situation of a large population following the Cannings models (Cannings 1974).  
 285 In this case the coalescent process is fully determined by the effective population size  $N_e = N/\sigma^2$   
 286 as previously noted (Kingman 1982a), where  $N$  is the population size and  $\sigma^2$  is the variance in the  
 287 number of offspring. Consequently there is a full tradeoff between  $N$  and  $\sigma^2$ , so that the ratio  $N_e$  can  
 288 be estimated but not the parameters  $N$  and  $\sigma^2$  separately.

## 289 8 Implementation

290 We implemented the analytical methods described in this paper in a new R package entitled *EpiLambda*  
 291 which is available at <https://github.com/xavierdidelot/EpiLambda> for R version 3.5 or later. All  
 292 code and data needed to replicate the results are included in the “run” directory of the *EpiLambda*  
 293 repository. The R package **ape** was used to store, manipulate and visualise phylogenetic trees (Paradis  
 294 and Schliep 2019).

## 295 9 Discussion

296 We have described an ancestral process for infectious diseases which is relevant to the analysis of  
 297 outbreaks of a relatively small size, and to diseases with transmission heterogeneity. We have shown  
 298 how this process can be incorporated into a new Lambda-coalescent which we called the Omega-  
 299 coalescent. We only considered the situation where all samples are taken at the same time, but the  
 300 Omega-coalescent could be extended to allow temporally offset leaves following similar work on the  
 301 coalescent (Drummond et al. 2003) and the Beta-coalescent (Hoscheit and Pybus 2019). We also made  
 302 the simplifying assumption of a constant population size, but this could be relaxed following the same  
 303 approach as previously described for integrating variable population size into the coalescent (Griffiths  
 304 and Tavaré 1994; Pybus et al. 2000; Ho and Shapiro 2011) and the Beta-coalescent (Hoscheit and

Pybus 2019; Zhang and Palacios 2024). Allowing the population size to vary could be especially useful for the Omega-coalescent for several reasons. Firstly, since it is aimed at relatively small outbreaks, it is likely that their sizes varies significantly. Secondly, the probability of multiple merger events of various sizes depends explicitly on the population size in Equation 21. Changes in population size will therefore have an effect on the distribution of events observed, as can be seen for example in Figure 3. Thirdly, joint inference of a varying population size could help break the otherwise difficult joint inference of a fixed population size with the dispersion parameter (Figure 6).

We compared the Omega-coalescent only to the Beta-coalescent (Schweinsberg 2003) in Figure 3 as it is the model that has been most frequently used for infectious diseases (Hoscheit and Pybus 2019; Menardo et al. 2021; Helekal et al. 2025). Several other Lambda-coalescent models have been proposed previously, such as the Dirac coalescent (Eldon and Wakeley 2006), the Durrett-Schweinsberg coalescent (Durrett and Schweinsberg 2005) or the extended Beta-coalescent (Helekal et al. 2025). However, none of these models is equivalent to the Omega-coalescent model. Indeed these previously described Lambda-coalescent models are mostly concerned with situations where an individual can be the father of a significant portion of a population in spite of the population being large, as opposed to the small populations with superspreading we considered here. The xi-coalescent models are extensions to the Lambda-coalescent models that admit multiple simultaneous mergers (Schweinsberg 2000). This is clearly relevant to our basic discrete time model for small outbreaks, since in small populations it is quite likely that separate subsets of individuals have the same infector in the previous generation. However the exact timing of ancestry events is never available so that we must rely on ancestral dating estimation with no notion of event co-occurrence (Volz and Frost 2017; Didelot et al. 2018; Bouckaert et al. 2019; Helekal et al. 2025). We therefore introduced a continuous time approximation in Equation 29 so that ancestry events do not co-occur. The exact coalescent process for the discrete time Wright-Fisher process in a small population has been previously described (Fu 2006). It would be difficult however to extend this approach to the more complex forward-in-time model we considered here, with variable population size and specific offspring distribution, which further justifies our continuous time approximation.

Finally, it should be noted that our model describes the transmission tree during an outbreak, which is different from a phylogeny (Jombart et al. 2011). This difference is often ignored and in some settings it might be appropriate to do so, but not always. Consequently, some previous studies have used models of within-host evolution to bridge the gap between transmission and phylogenetic trees (Didelot et al. 2014; Hall et al. 2015; Didelot et al. 2017). However, these models assume that each transmission event happens independently from one infector to each of its infectees. This is not necessarily true



338 especially when considering superspreading events in which many individuals can become infected  
339 simultaneously (Riley et al. 2003; Wallinga and Teunis 2004; Ho et al. 2023; Craddock et al. 2025).  
340 In conclusion, we have described a new ancestral model for infectious disease outbreaks, which we  
341 hope will be useful especially in settings where the outbreaks are small or in the presence of high  
342 transmission heterogeneity.

## 343 **Acknowledgements**

344 We acknowledge funding from the National Institute for Health Research (NIHR) Health Protection  
345 Research Unit in Genomics and Enabling Data.

## References

- Anderson, R.M., May, R.M., 1991. *Infectious Diseases of Humans: Dynamics and Control*. Oxford University Press, USA.
- Berestycki, N., 2009. Recent progress in coalescent theory. *arXiv* , 0909.3985.
- Bouckaert, R., Vaughan, T.G., Fourment, M., Gavryushkina, A., Heled, J., Denise, K., Maio, N.D., Matschiner, M., Ogilvie, H., Plessis, L., Poppinga, A., 2019. BEAST 2.5 : An Advanced Software Platform for Bayesian Evolutionary Analysis. *PLoS computational biology* 15, e1006650.
- Brent, R.P., 1971. An algorithm with guaranteed convergence for finding a zero of a function. *The computer journal* 14, 422–425.
- Byrd, R.H., Lu, P., Nocedal, J., Zhu, C., 1995. A limited memory algorithm for bound constrained optimization. *SIAM Journal on scientific computing* 16, 1190–1208.
- Cannings, C., 1974. The latent roots of certain Markov chains arising in genetics: a new approach, I. Haploid models. *Adv. Appl. Probab.* 6, 260–290.
- Craddock, H., Spencer, S.E., Didelot, X., 2025. A bayesian modelling framework with model comparison for epidemics with super-spreading. *arXiv* , 2501.12768.
- Didelot, X., Croucher, N.J., Bentley, S.D., Harris, S.R., Wilson, D.J., 2018. Bayesian inference of ancestral dates on bacterial phylogenetic trees. *Nucleic Acids Research* 46, e134–e134.
- Didelot, X., Fraser, C., Gardy, J., Colijn, C., 2017. Genomic infectious disease epidemiology in partially sampled and ongoing outbreaks. *Molecular Biology and Evolution* 34, 997–1007.
- Didelot, X., Gardy, J., Colijn, C., 2014. Bayesian inference of infectious disease transmission from whole genome sequence data. *Molecular Biology and Evolution* 31, 1869–1879.
- Didelot, X., Urwin, R., Maiden, M.C.J., Falush, D., 2009. Genealogical typing of *Neisseria meningitidis*. *Microbiology* 155, 3176–86.
- Donnelly, P., Kurtz, T.G., 1999. Particle Representations for Measure-Valued Population Models. *The Annals of Probability* 27.
- Drummond, A.J., Pybus, O.G., Rambaut, A., Forsberg, R., Rodrigo, A.G., 2003. Measurably evolving populations. *Trends in Ecology and Evolution* 18, 481–488.

373 Du, Z., Wang, C., Liu, C., Bai, Y., Pei, S., Adam, D.C., Wang, L., Wu, P., Lau, E.H.Y., Cowling,  
 374 B.J., 2022. Systematic review and meta-analyses of superspreading of SARS-CoV-2 infections.  
 375 *Transboundary and Emerging Diseases* 69.

376 Durrett, R., Schweinsberg, J., 2005. A coalescent model for the effect of advantageous mutations on  
 377 the genealogy of a population. *Stochastic Processes and their Applications* 115, 1628–1657.

378 Eldon, B., Wakeley, J., 2006. Coalescent Processes When the Distribution of Offspring Number Among  
 379 Individuals Is Highly Skewed. *Genetics* 172, 2621–2633.

380 Ferguson, N.M., Cummings, D.A.T., Fraser, C., Cajka, J.C., Cooley, P.C., Burke, D.S., 2006. Strategies  
 381 for mitigating an influenza pandemic. *Nature* 442, 448–452.

382 Fiala, K.L., Sokal, R.R., 1985. Factors determining the accuracy of cladogram estimation: Evolution  
 383 using computer simulation. *Evolution* 39, 609–622.

384 Fisher, R.A., 1930. *The genetical theory of natural selection*. Clarendon Press.

385 Fraser, C., Li, L.M., 2017. Coalescent models for populations with time-varying population sizes and  
 386 arbitrary offspring distributions. *bioRxiv* , 10.1101/131730.

387 Fraser, C., Riley, S., Anderson, R.M., Ferguson, N.M., 2004. Factors that make an infectious disease  
 388 outbreak controllable. *Proceedings of the National Academy of Sciences* 101, 6146–6151.

389 Fu, Y.X., 2006. Exact coalescent for the Wright–Fisher model. *Theoretical Population Biology* 69,  
 390 385–394.

391 Gómez-Carballa, A., Pardo-Seco, J., Bello, X., Martínón-Torres, F., Salas, A., 2021. Superspreading  
 392 in the emergence of COVID-19 variants. *Trends in Genetics* 37, 1069–1080.

393 Grassly, N.C., Fraser, C., 2008. Mathematical models of infectious disease transmission. *Nature*  
 394 *Reviews Microbiology* 6, 477–87.

395 Griffiths, R.C., Tavaré, S., 1994. Sampling theory for neutral alleles in a varying environment.  
 396 *Philosophical Transactions of the Royal Society B* 344, 403–410.

397 Hall, M., Woolhouse, M., Rambaut, A., 2015. Epidemic Reconstruction in a Phylogenetics Framework:  
 398 Transmission Trees as Partitions of the Node Set. *PLOS Computational Biology* 11, e1004613.

399 Heledal, D., Koskela, J., Didelot, X., 2025. Inference of multiple mergers while dating a pathogen  
 400 phylogeny. *Systematic Biology* , syaf003.

401 Ho, F., Parag, K.V., Adam, D.C., Lau, E.H.Y., Cowling, B.J., Tsang, T.K., 2023. Accounting for the  
402 Potential of Overdispersion in Estimation of the Time-varying Reproduction Number. *Epidemiology*  
403 34, 201–205.

404 Ho, S.Y.W., Shapiro, B., 2011. Skyline-plot methods for estimating demographic history from  
405 nucleotide sequences. *Molecular Ecology Resources* 11, 423–434.

406 Hoscheit, P., Pybus, O.G., 2019. The multifurcating skyline plot. *Virus Evolution* 5, 1–10.

407 Jombart, T., Eggo, R.M., Dodd, P.J., Balloux, F., 2011. Reconstructing disease outbreaks from genetic  
408 data: A graph approach. *Heredity* 106, 383–90.

409 Keeling, M.J., Rohani, P., 2008. Modeling infectious diseases in humans and animals. Princeton  
410 university press.

411 Kingman, J., 1982a. The coalescent. *Stochastic Processes and their Applications* 13, 235–248.

412 Kingman, J.F.C., 1982b. On the genealogy of large populations. *Journal of Applied Probability* 19,  
413 27–43.

414 Koelle, K., Rasmussen, D.A., 2012. Rates of coalescence for common epidemiological models at  
415 equilibrium. *Journal of The Royal Society Interface* 9, 997–1007.

416 Koskela, J., 2018. Multi-locus data distinguishes between population growth and multiple merger  
417 coalescents. *Statistical Applications in Genetics and Molecular Biology* 17, 1–24.

418 Kucharski, A.J., Althaus, C.L., 2015. The role of superspreading in Middle East respiratory syndrome  
419 coronavirus (MERS-CoV) transmission. *Eurosurveillance* 20, 14–18.

420 Lemieux, J.E., Siddle, K.J., Shaw, B.M., Loreth, C., Schaffner, S.F., Gladden-Young, A., Adams,  
421 G., Fink, T., Tomkins-Tinch, C.H., Krasilnikova, L.A., DeRuff, K.C., Rudy, M., Bauer, M.R.,  
422 Lagerborg, K.A., Normandin, E., Chapman, S.B., Reilly, S.K., Anahtar, M.N., Lin, A.E., Carter,  
423 A., Myhrvold, C., Kembball, M.E., Chaluvadi, S., Cusick, C., Flowers, K., Neumann, A., Cerrato,  
424 F., Farhat, M., Slater, D., Harris, J.B., Branda, J.A., Hooper, D., Gaeta, J.M., Baggett, T.P.,  
425 O’Connell, J., Gnirke, A., Lieberman, T.D., Philippakis, A., Burns, M., Brown, C.M., Luban, J.,  
426 Ryan, E.T., Turbett, S.E., LaRocque, R.C., Hanage, W.P., Gallagher, G.R., Madoff, L.C., Smole, S.,  
427 Pierce, V.M., Rosenberg, E., Sabeti, P.C., Park, D.J., MacInnis, B.L., 2021. Phylogenetic analysis  
428 of SARS-CoV-2 in Boston highlights the impact of superspreading events. *Science* 371, eabe3261.

429 Li, L.M., Grassly, N.C., Fraser, C., 2017. Quantifying Transmission Heterogeneity Using Both  
430 Pathogen Phylogenies and Incidence Time Series. *Molecular Biology and Evolution* 34, 2982–2995.

431 Lloyd-Smith, J., Schreiber, S., Kopp, P., Getz, W., 2005. Superspreading and the effect of individual  
432 variation on disease emergence. *Nature* 438, 355–9.

433 Menardo, F., Gagneux, S., Freund, F., 2021. Multiple Merger Genealogies in Outbreaks of  
434 *Mycobacterium tuberculosis*. *Molecular Biology and Evolution* 38, 290–306.

435 Miró Pina, V., Joly, É., Siri-Jégousse, A., 2023. Estimating the Lambda measure in multiple-merger  
436 coalescents. *Theoretical Population Biology* 154, 94–101.

437 Moran, P., 1958. Random Processes in Genetics. *Mathematical Proceedings of the Cambridge*  
438 *Philosophical Society* 54, 60–71.

439 Paradis, E., Schliep, K., 2019. Ape 5.0: An environment for modern phylogenetics and evolutionary  
440 analyses in R. *Bioinformatics* 35, 526–528.

441 Pitman, J., 1999. Coalescents with multiple collisions. *The Annals of Probability* 27, 1870–1902.

442 Potts, R.B., 1953. Note on the Factorial Moments of Standard Distributions. *Australian Journal of*  
443 *Physics* 6, 498–499.

444 Pybus, O.G., Rambaut, A., Harvey, P.H., 2000. An integrated framework for the inference of viral  
445 population history from reconstructed genealogies. *Genetics* 155, 1429–1437.

446 Riley, S., Fraser, C., a Donnelly, C., Ghani, A.C., Abu-Raddad, L.J., Hedley, A.J., Leung, G.M., Ho,  
447 L.M., Lam, T.H., Thach, T.Q., Chau, P., Chan, K.P., Lo, S.V., Leung, P.Y., Tsang, T., Ho, W., Lee,  
448 K.H., Lau, E.M.C., Ferguson, N.M., Anderson, R.M., 2003. Transmission dynamics of the etiological  
449 agent of SARS in Hong Kong: Impact of public health interventions. *Science* 300, 1961–6.

450 Sagitov, S., 1999. The general coalescent with asynchronous mergers of ancestral lines. *Journal of*  
451 *Applied Probability* 36, 1116–1125.

452 Schweinsberg, J., 2000. Coalescents with Simultaneous Multiple Collisions. *Electronic Journal of*  
453 *Probability* 5.

454 Schweinsberg, J., 2003. Coalescent processes obtained from supercritical Galton–Watson processes.  
455 *Stochastic Processes and their Applications* 106, 107–139.

456 Stein, R.A., 2011. Super-spreaders in infectious diseases. *International Journal of Infectious Diseases*  
457 15, e510–e513.

458 Svensson, A., 2007. A note on generation times in epidemic models. *Mathematical Biosciences* 208(1),  
459 300–311.

460 Tripathi, R.C., Gupta, R.C., Gurland, J., 1994. Estimation of parameters in the beta binomial model.  
 461 *Annals of the Institute of Statistical Mathematics* 46, 317–331.

462 Volz, E.M., 2012. Complex population dynamics and the coalescent under neutrality. *Genetics* 190,  
 463 187–201.

464 Volz, E.M., Frost, S.D.W., 2017. Scalable relaxed clock phylogenetic dating. *Virus Evolution* 3, vex025.

465 Wallinga, J., Teunis, P., 2004. Different Epidemic Curves for Severe Acute Respiratory Syndrome  
 466 Reveal Similar Impacts of Control Measures. *American Journal of Epidemiology* 160, 509–516.

467 Wang, J., Chen, X., Guo, Z., Zhao, S., Huang, Z., Zhuang, Z., Wong, E.L.y., Zee, B.C.Y., Chong,  
 468 M.K.C., Wang, M.H., Yeoh, E.K., 2021. Superspreading and heterogeneity in transmission of SARS,  
 469 MERS, and COVID-19: A systematic review. *Computational and Structural Biotechnology Journal*  
 470 19, 5039–5046.

471 Wang, L., Didelot, X., Yang, J., Wong, G., Shi, Y., Liu, W., Gao, G.F., Bi, Y., 2020. Inference of  
 472 person-to-person transmission of COVID-19 reveals hidden super-spreading events during the early  
 473 outbreak phase. *Nature Communications* 11, 5006.

474 Woolhouse, M.E.J., Dye, C., Etard, J.F., Smith, T., Charlwood, J.D., Garnett, G.P., Hagan, P., Hii,  
 475 J.L.K., Ndhlovu, P.D., Quinnell, R.J., Watts, C.H., Chandiwana, S.K., Anderson, R.M., 1997.  
 476 Heterogeneities in the transmission of infectious agents: Implications for the design of control  
 477 programs. *Proceedings of the National Academy of Sciences* 94, 338–342.

478 Wright, S., 1931. Evolution in Mendelian populations. *Genetics* 16, 97–159.

479 Zhang, J., Palacios, J.A., 2024. Multiple merger coalescent inference of effective population size. *arXiv*  
 480 , 2407.14976.